

Disruption of Scaffold Attachment Factor B1 Leads to TBX2 Up-regulation, Lack of p19^{ARF} Induction, Lack of Senescence, and Cell Immortalization

Klaudia M. Dobrzycka,¹ Kaiyan Kang,¹ Shiming Jiang,¹ Rene Meyer,¹ Pulivarthi H. Rao,² Adrian V. Lee,¹ and Steffi Oesterreich¹

¹Departments of Medicine and Molecular and Cellular Biology, The Breast Center and ²Texas Children's Cancer Center, Baylor College of Medicine, Houston, Texas

Abstract

Scaffold attachment factor B1 (SAFB1) is a multifunctional protein, which has previously been implicated in breast cancer. Here, we show that genetic deletion of SAFB1 in mouse embryonic fibroblasts (MEF) leads to spontaneous immortalization and altered expression of two proteins involved in immortalization and escape from senescence: low levels of p19^{ARF} and high levels of TBX2. Inactivation of TBX2 using a dominant-negative TBX2 resulted in up-regulation of p19^{ARF} in SAFB1 knockout MEFs. SAFB1 loss also caused lack of contact inhibition, increased foci formation, and increased oncogene-induced anchorage-independent growth. These findings suggest that SAFB1 is a novel player in cellular immortalization and transformation. (Cancer Res 2006; 66(16): 7859-63)

Introduction

Scaffold attachment factor B1 (SAFB1) is a nuclear protein involved in RNA processing, transcriptional regulation, chromatin organization, and stress response (1). The protein contains numerous highly conserved functional domains. SAFB1 can bind RNA via a RNA recognition motif (2) and is found in complexes with RNA processing proteins (3, 4). Because SAFB1 can also interact with RNA polymerase II, it has been suggested to be part of a "transcriptosome" complex (3). The NH₂ terminus harbors a SAF-Box, a homeodomain-like DNA-binding motif that interacts with scaffold/matrix attachment regions (S/MAR; ref. 5). In addition, an independent repression domain is located at the COOH terminus (6).

Previous studies suggested that SAFB1 plays an important role in human breast cancer. It functions as an estrogen receptor α (ER α) corepressor by directly binding to ER α and inhibiting its transcriptional activity (7). SAFB1 maps to a chromosomal locus that displays unusually high rates of loss of heterozygosity in invasive breast cancers, and SAFB1 mutations have been identified in microdissected breast tumor tissue but not in the normal adjacent tissue (8).

We have recently generated SAFB1 knockout mice, which show high preneonatal and neonatal lethality, severe dwarfism associated with low insulin-like growth factor-I levels, and female subfertility and male infertility (9). Here, we show that mouse embryonic

fibroblasts (MEF) from SAFB1^{-/-} mice fail to undergo senescence and exhibit spontaneous immortalization, which was associated with a lack of p19^{ARF} induction and high levels of TBX2, a known p19^{ARF} repressor. SAFB1^{-/-} cells proliferate in growth-restricting conditions and show increased anchorage-independent growth in the presence of cooperating oncogenes. These findings place SAFB1 in a unique group of genes that are critical in cellular immortalization and transformation.

Materials and Methods

Cells and tissue culture. MEF pairs were obtained from sibling SAFB1^{+/+} and SAFB1^{-/-} embryos from the same mother as described previously (9), and experiments were repeated using other MEF pairs from different mothers. Short-term proliferation assays were done by plating 1×10^4 cells per well in 24-well plates in triplicates, and cells were counted daily. For foci formation assays, MEFs were plated at 1×10^6 in a 10-cm plate and cells were transiently transfected using Lipofect-AMINE (Invitrogen, Carlsbad, CA) with oncogenes. Medium was changed twice weekly, and foci were allowed to form for 2 to 3 weeks. To obtain stably transformed MEFs, cells were transfected and single colonies were expanded. To test anchorage-independent growth, MEFs were suspended in 0.4% SeaPlaque agar (Cambrex, East Rutherford, NJ) in the growth medium and overlaid on 0.8% agar in the same medium. Colonies were stained with 1 mg/mL 3-(4,5-dimethylthiazol-2-yl)-2,5-diphenyltetrazolium bromide (ICN, Irvine, CA) 2 weeks later and counted. Population doublings were calculated according to the formula $\log(\text{final cell number}/\text{plated cell number}) / \log_2$. Senescence-associated β -galactosidase (SA- β -gal) was measured by using a Senescence-associated β -galactosidase kit (Cell Signaling, Beverly, MA).

Protein and RNA analysis. Immunoblotting was done as described previously (2). The p19^{ARF} antibody was purchased from Abcam (Cambridge, United Kingdom), and the antibody recognizing mouse SAFB1 has been described previously (9).

For the reverse transcription-PCR (RT-PCR) analysis, total cellular RNA was isolated with RNeasy kit (Qiagen, Valencia, CA), RNA was reverse transcribed with SuperScript II RNase H Reverse Transcriptase (Invitrogen), and PCR was done using primers used for SAFB1 (9), p19^{ARF} (10), TBX2 (11), Bmi-1 (5'-TGTGTCCTGTGTGGAGGGTA-3' and 5'-TGGTTTGTGAACCTGGACA-3'), CBX7 (5'-TGTCAGCCATAGGCGAGCA-3' and 5'-AACTTTGCCCTCCGCACG-3'), and DMP1 (5'-CTGTAGCT-GAAAGAGTGGGTA-3' and 5'-TGTATTATCTTCCAAGCGGGC-3'). To measure TBX2 and TBX3 mRNA by quantitative PCR using an ABI PRISM 7700 (PE Applied Biosystems, Foster City, CA), RNA was DNase treated and reverse transcribed and cDNA was amplified for 40 cycles of 95°C for 12 seconds and 60°C for 1 minute. The change in expression was calculated by the $\Delta\Delta C_t$ method. The primers (mouse TBX2, 5'-TGAAGCTCCATACAGCACCTT-3' and 5'-TTGTGCGATCTTCAGCTGTGTAATCT-3'; mouse TBX3, 5'-CCACCTCAACAACACGTTCT-3' and 5'-TAAGGAAACAGGCTCCCGAA-3'; and mouse β -actin, 5'-GCTCTGGCTCCTAGCACCAT-3' and 5'-CCACCGATCCACACAGAGTAC-3') and Taqman probes (TBX2, TCTTCCCAGAGACCGACTTCATCGCTG; TBX3, CCTCCAGGGCTTGGCTATGTGCG; and β -actin, ATCAAGATCATGTCTCCTCCTGAGCGC) were purchased from

Requests for reprints: Steffi Oesterreich, The Breast Center, Baylor College of Medicine, One Baylor Plaza, BCM 600, Houston, TX 77030. Phone: 713-798-1623; Fax: 713-798-1642; E-mail: steffio@breastcenter.tmc.edu.

©2006 American Association for Cancer Research.

doi:10.1158/0008-5472.CAN-06-1381

Eurogentec (Philadelphia, PA) or Integrated DNA Technologies, Inc. (Coralville, IA).

Virus production and MEFs infection. 293T cells were transfected with ecotropic helper virus DNA (pCL-Eco) and either pBabe-p19^{ARF}, pBabe-rasV12, pBabe-control, or pBabe-dnTBX2 (12). Supernatants containing infectious retrovirus were harvested 24 to 72 hours after transfection, filtered, and stored on ice. MEFs were infected thrice for 3 to 4 hours each with virus-containing supernatant containing 10 µg/mL polybrene (Sigma, St. Louis, MO).

Results

SAFB1 deficiency leads to lack of senescence and immortalization. To analyze the effect of SAFB1 loss on tumorigenesis *in vitro*, we generated pairs of SAFB1^{+/+} and SAFB1^{-/-} MEFs and confirmed SAFB1 status by RT-PCR and Western blot (Fig. 1A). Growth curves using early passage MEFs revealed slightly slower growth of SAFB1^{-/-} MEFs compared with SAFB1^{+/+} MEFs (Fig. 1B).

Next, we determined the effect of SAFB1 loss on cellular senescence and immortalization by long-term passaging of MEFs obtained from three independent SAFB1^{+/+} and SAFB1^{-/-} embryos following the 3T3 protocol. As expected, SAFB1^{+/+} MEFs showed a decline in their proliferative rate at about passage 12 and ultimately underwent senescence (Fig. 1C). Of three SAFB1^{+/+}

MEFs analyzed, only one immortal population emerged after passage 28. After several attempts, we were also able to generate immortalized populations from the other two SAFB1^{+/+} MEFs. In contrast, all the SAFB1^{-/-}-independent MEFs did not lose proliferative capacity following serial passaging with increased proliferative potential that emerged at passages 12 to 16. This bypass of cellular senescence was easily observed microscopically. Early passage, exponentially growing SAFB1^{+/+} and SAFB1^{-/-} MEFs did not differ in cell morphology (Fig. 1D). In contrast, late passage SAFB1^{+/+} acquired a large, flattened cell morphology, characteristic of senescent cells, whereas SAFB1^{-/-} MEFs remained small and more refractile. This morphology change, together with the biphasic curves for the population doublings (MEF pairs 1 and 3), suggests that there is an outgrowth of a specific subgroup of MEFs. We further confirmed the lack of senescence by staining for SA-β-gal. Whereas SAFB1^{+/+} MEFs showed high levels of SA-β-gal activity, SAFB1^{-/-} MEFs showed decreased SA-β-gal activity at passages 8 and 15 (Fig. 1E). These data indicate that loss of SAFB1 results in immortalization by allowing MEFs to bypass cellular senescence.

Immortalization of SAFB1^{-/-} MEFs is associated with lack of p19^{ARF} induction and increased TBX2 levels. Next, we measured levels of p19^{ARF}, a known inducer of senescence in MEFs

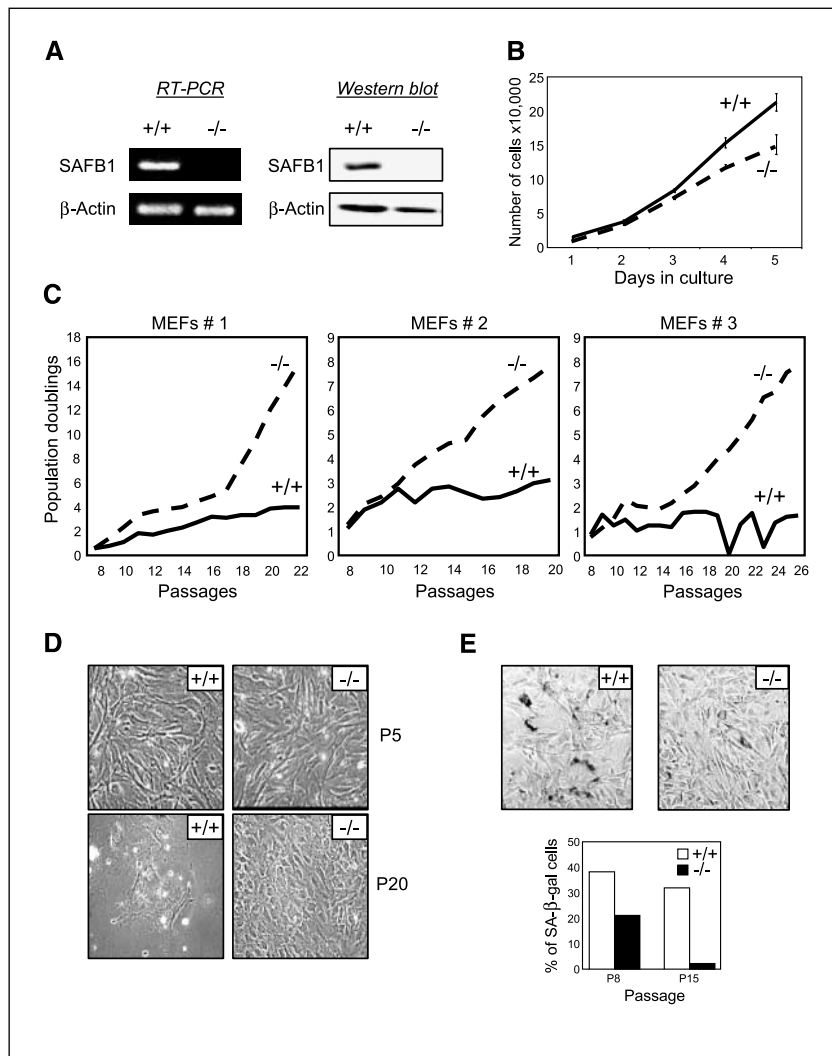


Figure 1. SAFB1^{-/-} MEFs fail to undergo senescence and spontaneously immortalize. *A*, RT-PCR and immunoblot analysis of SAFB1^{+/+} and SAFB1^{-/-} MEFs. β-Actin was used as a loading control. *B*, growth curve of primary MEFs (passage 5). *Points*, cell count from triplicate wells; *bars*, SE. Similar results were obtained with at least three independent MEF pairs. *C*, growth of MEFs passaged according to the 3T3 protocol. Accumulated number of population doublings of MEF pairs from three different mothers. *D*, *left*, representative phase-contrast images of MEFs at passages 5 and 20. *E*, *top*, expression of SA-β-gal in MEFs at passage 8; *bottom*, percentage of β-gal-positive MEFs was calculated and graphed for each genotype for passages 8 and 15.

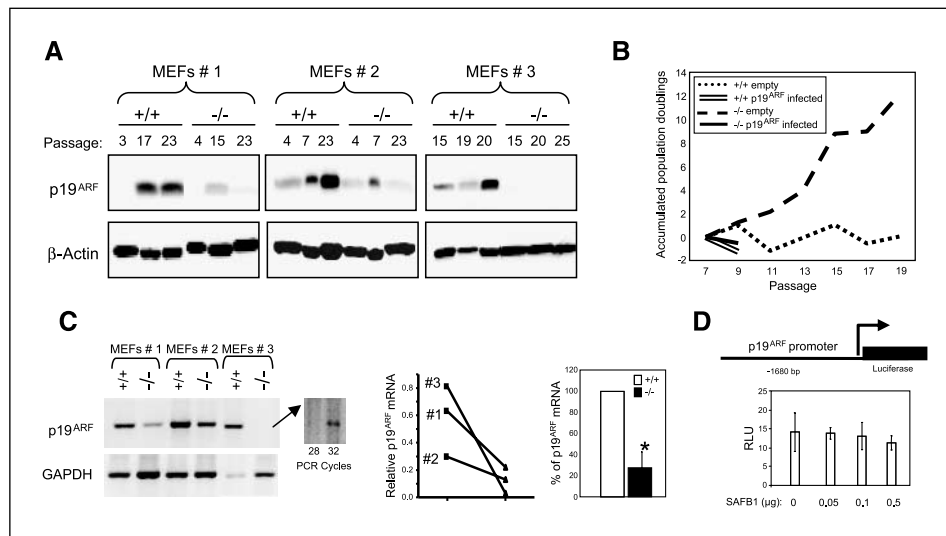
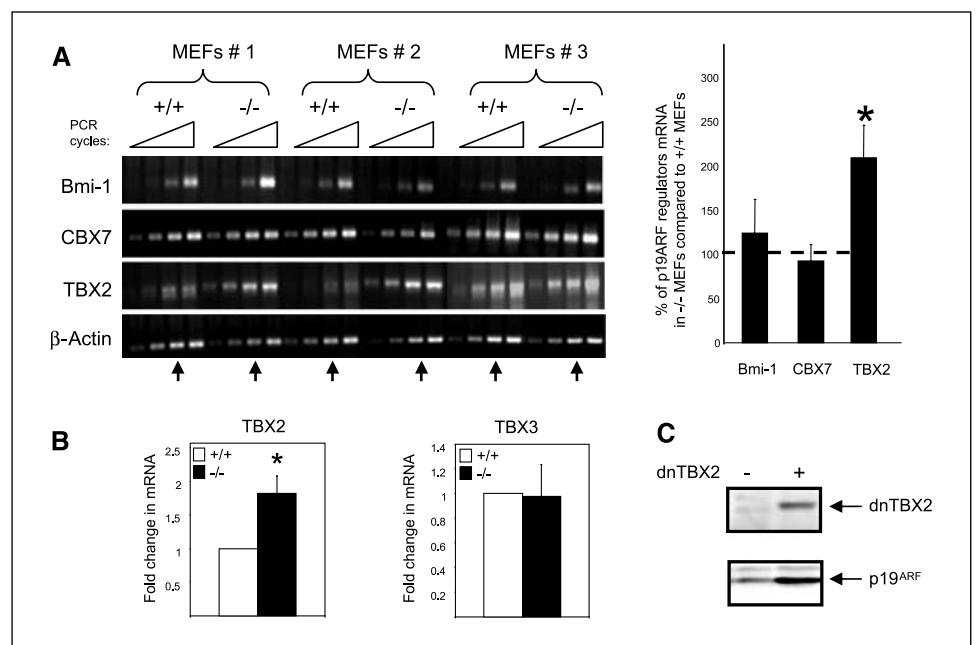


Figure 2. Lack of p19^{ARF} induction in SAFB1^{-/-} MEFs. *A*, immunoblot analysis of p19^{ARF} using protein lysates from three individual MEF pairs at indicated passages. β -Actin was used as loading control. *B*, reintroduction of p19^{ARF} into SAFB1^{+/+} and SAFB1^{-/-} MEFs. Cells at passage 7 were infected with virus delivering empty vector or p19^{ARF} and serially passaged following the 3T3 protocol. *C*, p19^{ARF} mRNA expression in SAFB1^{+/+} and SAFB1^{-/-} MEFs. p19^{ARF} was amplified from three MEF pairs [corresponding to (*A*)] by RT-PCR (26 cycles). For SAFB1^{-/-} MEF pair 3, the PCR cycle number needed to be increased to 32 to detect the PCR product. Graphical representation of densitometry from the RT-PCR shows relative p19^{ARF} mRNA [corrected for glyceraldehyde-3-phosphate dehydrogenase (*GAPDH*)] in a paired and nonpaired *t* test. *, *P* = 0.047. *D*, MEFs were transfected with a p19^{ARF}-Luc (-1,680 bp) reporter construct and SAFB1pcDNA1 as indicated, and relative luciferase unit (*RLU*) was determined.

(Fig. 2*A*; ref. 13). As expected, p19^{ARF} levels were induced with increased passaging of SAFB1^{+/+} MEFs. In contrast, we found unusually low p19^{ARF} levels in SAFB1^{-/-} MEFs; pairs 1 and 2 showed very weak p19^{ARF} induction and no p19^{ARF} protein was detected in pair 3 even after prolonged exposure. Reintroduction of p19^{ARF} into SAFB1^{-/-} cells by retroviral infection resulted in growth arrest, whereas cells infected with empty virus maintained constant growth and did not undergo senescence (Fig. 2*B*). These findings strongly suggest that the lack of senescence in SAFB1^{-/-} cells was due to lack of p19^{ARF} induction and that other downstream effectors of p19^{ARF} were not inactivated.

To determine whether p19^{ARF} protein changes were also reflected by changes at the mRNA level, we measured p19^{ARF} mRNA and detected significant decreases in all three SAFB1^{-/-} MEFs compared with SAFB1^{+/+} (Fig. 2*C*). In SAFB1^{-/-} MEF pair 3, which did not express p19^{ARF} protein, we detected very low mRNA, suggesting that the genomic locus was intact in all SAFB1^{-/-} MEFs. We did not detect any effect of SAFB1 on a p19^{ARF} promoter (-1,680 bp) activity using transient reporter assays in MEFs (Fig. 2*D*) and in MCF-7 cells (data not shown), suggesting that it was unlikely that SAFB1 directly regulates expression of p19^{ARF} transcription. We therefore hypothesized that SAFB1 may indirectly

Figure 3. Increased TBX2 levels in SAFB1^{-/-} MEFs. *A*, expression levels of repressors of p19^{ARF} levels in three independent MEF pairs. Semiquantitative RT-PCR was done for Bmi-1, CBX7, and TBX2 using increasing number of PCR cycles (Bmi-1, 15, 18, 21, and 24; CBX7, 30, 33, 36, and 39; and TBX2, 29, 32, 35, and 38) with β -actin (cycle numbers 15, 18, 21, and 24) as a control. Arrow, band intensities were quantified at one cycle. Ratio of SAFB1^{-/-} to SAFB1^{+/+}. Columns, mean of three independent MEF pairs; bars, SD. *, *P* = 0.0078, two-tailed *t* test. *B*, analysis of TBX2 and TBX3 mRNA in primary SAFB1^{-/-} MEFs. TBX2 and TBX3 mRNA levels in MEFs (*n* = 6) were measured by quantitative PCR. Relative mRNA levels corrected for β -actin. *, *P* = 0.0281, two-tailed paired *t* test. Columns, mean (*n* = 6); bars, SE. *C*, dominant-negative TBX2 (*dnTBX2*) up-regulates p19^{ARF} expression. SAFB1^{-/-} MEFs were infected with pBabe-dnTBX2, and protein expression of dominant-negative TBX2 and p19^{ARF} was analyzed using hemagglutinin and p19^{ARF} antibodies, respectively.



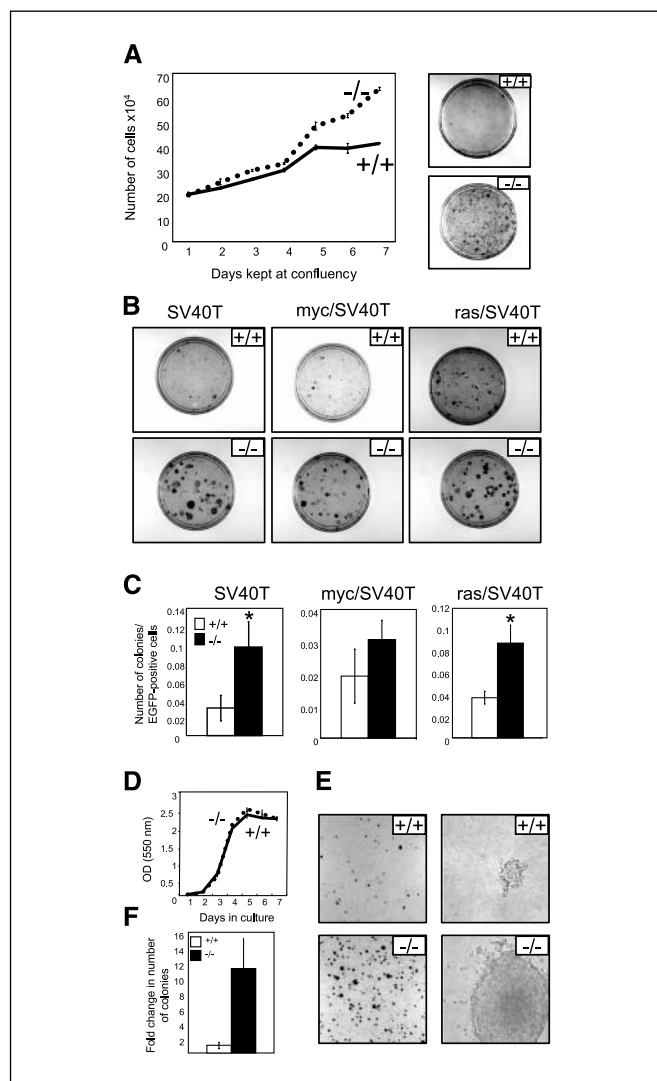


Figure 4. Lack of SAFB1 leads to a partially transformed phenotype. **A**, postconfluent growth of MEFs. *Left*, SAFB1^{+/+} and SAFB1^{-/-} MEFs (passage 7) were plated at confluency, and growth was measured. *Points*, mean of experiments done in triplicate; *bars*, SE. Similar results were obtained in two independent experiments. *Right*, SAFB1^{+/+} and SAFB1^{-/-} MEFs (passage 10) were kept at confluency for 3 to 4 weeks. Pictures are representative of three independent experiments. **B**, anchorage-dependent, oncogene-induced (SV40T, myc/SV40T, and ras/SV40T) foci formation assay in primary MEFs. Similar results were obtained in at least three independent experiments. **C**, quantitative analysis of anchorage-dependent, oncogene-induced (SV40T, myc/SV40T, and ras/SV40T) foci formation assay in primary MEFs ($n = 3$ per genotype). *Columns*, mean foci number of three clones corrected for number of fluorescent cells (to correct for transfection efficiency); *bars*, SE. *, $P < 0.05$. **D**, growth properties of MEFs stably transformed with ras/SV40T. Representative growth curves for three independent transformed MEF clones for each genotype. *Points*, mean of experiments done in triplicate; *bars*, SE. **E**, anchorage-independent growth of SAFB1^{+/+} and SAFB1^{-/-} MEFs stably transformed with ras/SV40T. Pictures at low (*left*) and high (*right*) magnifications. **F**, *columns*, mean of three independent clones shown as fold change compared with SAFB1^{+/+}; *bars*, SE.

affect p19^{ARF} expression by inhibiting a p19^{ARF} repressor, such as Bmi-1 (14), CBX7 (15), or TBX2 (16). RT-PCR analysis revealed that there was no difference in expression of Bmi-1 and CBX7; however, TBX2 was significantly increased in SAFB1^{-/-} MEFs (Fig. 3A). TBX2 overexpression was confirmed by quantitative PCR using additional MEF pairs (Fig. 3B). Expression of *TBX3*, a gene that has also been shown to regulate p19^{ARF} and senescence (17),

was not altered (Fig. 3B), suggesting that SAFB1 specifically regulates expression of TBX2. This regulation was not at the level of RNA stability because we did not detect a difference in TBX2 RNA half-life between SAFB1^{+/+} and SAFB1^{-/-} MEFs (data not shown).

Overexpression of a dominant-negative TBX2, previously described by Vance et al. (12), into SAFB1^{-/-} MEFs resulted in up-regulation of p19^{ARF} (Fig. 3C). Together, these findings provide support for a model, in which SAFB1 loss results in increased TBX2 expression associated with lack of induction of p19^{ARF} and thus lack of senescence and spontaneous immortalization.

Loss of SAFB1 leads to features of transformed phenotype.

Attainment of cell immortality is a prerequisite for transformation (18), and several MEF models, which undergo spontaneous immortalization, also display increased transformation capabilities. To determine whether SAFB1^{-/-} MEFs showed increased transformation characteristics, we tested their ability to proliferate in growth-restricting conditions. When cells were grown at confluency, SAFB1^{+/+} MEFs showed contact inhibition and were growth arrested (days 5-7), whereas SAFB1^{-/-} MEFs continued to proliferate and achieved a higher density cellular monolayer (Fig. 4A, *left*). This loss of contact inhibition was even more pronounced when confluent cells were cultured long term (4 weeks), resulting in formation of multiple foci in SAFB1^{-/-} MEFs (Fig. 4A, *right*).

MEFs lacking p19^{ARF} fail to undergo senescence provoked by constitutive signaling of oncogenic ras (19) but are instead transformed. Infection of SAFB1^{-/-} MEFs with rasV12 did not result in full transformation (data not shown); thus, loss of SAFB1 alone does not cooperate with ras in cellular transformation. In contrast, overexpression of SV40T, myc/SV40T, or ras/SV40T resulted in increased number and size of foci (Fig. 4B), suggesting that SAFB1 loss results in increased efficiency of transformation by cooperating oncogenes. To determine whether number of foci was also increased in SAFB1^{-/-} MEFs, we cotransfected the oncogenes with enhanced green fluorescent protein (EGFP) and corrected the numbers of foci for the number of EGFP-positive cells. Overexpression of SV40T and ras/SV40T resulted in increased number of foci as shown in Fig. 4C.

We also generated stable clones of ras/SV40-transformed SAFB1^{-/-} and SAFB1^{+/+} cells. There was no difference in anchorage-dependent growth between ras/SV40T-transformed SAFB1^{-/-} and SAFB1^{+/+} cells (Fig. 4D; $n = 3$ per genotype). However, anchorage-independent growth in soft agar was dramatically increased as a consequence of SAFB1 loss in the stable clones (Fig. 4E and F). These data provide further evidence that loss of SAFB1 results in increased transformed phenotypes.

Discussion

Here, we provide critical data about the role of SAFB1 in cellular immortalization and transformation. MEFs lacking SAFB1 show altered expression of two proteins involved in the senescence and immortalization processes: low levels of p19^{ARF} and high levels of TBX2, a known repressor of p19^{ARF}. Although SAFB1^{-/-} MEFs are not fully transformed, they are able to proliferate in growth-restricting conditions and show increased anchorage-independent growth in the presence of oncogenes.

The failure of SAFB1^{-/-} MEFs to senesce and, as a consequence, to undergo spontaneous immortalization places SAFB1 into a unique set of genes regulating this process (20). We show that loss of SAFB1 leads to a reduction in p19^{ARF} levels but not to a

complete abrogation of expression. This effect was not direct, but indirect, possibly caused by increased expression of TBX2. TBX2 is a T-box transcription factor, which has been shown to repress p19^{ARF} promoter activity and whose overexpression leads to cell immortalization (16, 17). Indeed, inactivation of TBX2 using a dominant-negative TBX2 construct resulted in up-regulation of p19^{ARF}, providing strong support for a model, in which loss of SAFB1 causes an increase in TBX2 levels that in turn down-regulate p19^{ARF} promoter activity. The question remains as how SAFB1 regulates TBX2 expression. Preliminary experiments in our laboratory failed to establish a direct link in transient assays, suggesting a more complicated mechanism, which will be the focus of our future studies. An interesting possibility is that SAFB1 regulates TBX2 expression through effects on chromatin organization because the TBX2 5'-regulatory region contains a S/MAR, a consensus element that can be recognized by SAFB1.

Immortalization requires either biallelic loss of p19^{ARF} or inactivation of p53. For instance, p19^{ARF} heterozygous MEFs do not immortalize unless they lose the second allele (19). Interestingly, SAFB1^{-/-} MEFs are able to immortalize despite incomplete loss of p19^{ARF} expression. This suggests that loss of SAFB1 causes additional changes in as-yet-unknown target genes that cooperate with low p19^{ARF} levels in immortalization. Such genes are unlikely to be downstream effectors of p19^{ARF} (including p53) because reintroduction of p19^{ARF} into SAFB1^{-/-} MEFs readily inhibits cell proliferation, as one would expect from a functional p19^{ARF}-p53 pathway.

Previous work from the DePinho group has established that p19^{ARF} and p16INK4a loss do not cooperate with T antigen in MEF transformation (21). Therefore, our findings that loss of SAFB1 cooperates with T antigen support the notion from above that loss of SAFB1 may cause additional p19^{ARF}-independent alterations.

Collectively, our data suggest that loss of SAFB1 facilitates immortalization of primary MEFs and increased cell transformation. Our study is particularly important because it connects a gene involved in breast tumorigenesis to the senescence process. Ongoing and future experiments will determine whether the mechanism(s) by which SAFB1 interferes with the senescence program in MEFs is also conserved in human cells.

Acknowledgments

Received 4/14/2006; revised 6/14/2006; accepted 6/28/2006.

Grant support: NIH grant R01 CA92713 (S. Oesterreich), NIH Program Project grant P01 CA030195 [C.K. Osborne (principal investigator) and S. Oesterreich (project leader)], and Department of Defense Breast Cancer Award W81XWH 04-01-0423. K.M. Dobrzycka and S. Jiang were supported by the Department of Defense Breast Cancer Traineeship Awards W81XWH-04-1-0355 and DAMD 17-03-01-0323.

The costs of publication of this article were defrayed in part by the payment of page charges. This article must therefore be hereby marked *advertisement* in accordance with 18 U.S.C. Section 1734 solely to indicate this fact.

We thank Drs. Sherr (St. Jude Children's Research Hospital, Memphis, TN) and van Lohuizen (the Netherlands Cancer Institute, Amsterdam, the Netherlands) for the p19^{ARF} promoter plasmids, Dr. Lowe (Cold Spring Harbor Laboratory, New York, NY) for the rasV12 plasmid, Dr. Goding for the TBX2 plasmid (Marie Curie Research Institute, Surrey, United Kingdom), Dr. Hilsenbeck for help with statistical analysis, Dr. Ivanova and Ora Britton for outstanding animal care, and Dr. Chamness for critical reading and editing of the article.

References

- Oesterreich S. Scaffold attachment factors SAFB1 and SAFB2: innocent bystanders or critical players in breast tumorigenesis? *J Cell Biochem* 2003;90:653-61.
- Townson SM, Dobrzycka KM, Lee AV, et al. SAFB2, a new scaffold attachment factor homolog and estrogen receptor corepressor. *J Biol Chem* 2003;278:20059-68.
- Nayler O, Stratling W, Bourquin JP, et al. SAF-B protein couples transcription and pre-mRNA splicing to SAR/MAR elements. *Nucleic Acids Res* 1998;26:3542-9.
- Weighardt F, Cobianchi F, Cartegni L, et al. A novel hnRNP protein (HAP/SAF-B) enters a subset of hnRNP complexes and relocates in nuclear granules in response to heat shock. *J Cell Sci* 1999;112:1465-76.
- Kipp M, Gohring F, Ostendorp T, et al. SAF-Box, a conserved protein domain that specifically recognizes scaffold attachment region DNA. *Mol Cell Biol* 2000;20:7480-9.
- Townson SM, Kang K, Lee AV, Oesterreich S. Structure-function analysis of the estrogen receptor α corepressor scaffold attachment factor-B1: identification of a potent transcriptional repression domain. *J Biol Chem* 2004;279:26074-81.
- Oesterreich S, Zhang Q, Hopp T, et al. Tamoxifen-bound estrogen receptor (ER) strongly interacts with the nuclear matrix protein HET/SAF-B, a novel inhibitor of ER-mediated transactivation. *Mol Endocrinol* 2000;14:369-81.
- Oesterreich S, Allred DC, Mohsin SK, et al. High rates of loss of heterozygosity on chromosome 19p13 in human breast cancer. *Br J Cancer* 2001;84:493-8.
- Ivanova M, Dobrzycka KM, Jiang S, et al. Scaffold attachment factor b1 functions in development, growth, and reproduction. *Mol Cell Biol* 2005;25:2995-3006.
- Quelle DE, Zindy F, Ashmun RA, Sherr CJ. Alternative reading frames of the INK4a tumor suppressor gene encode two unrelated proteins capable of inducing cell cycle arrest. *Cell* 1995;83:993-1000.
- Bollag RJ, Siegfried Z, Cebra-Thomas JA, et al. An ancient family of embryonically expressed mouse genes sharing a conserved protein motif with the T locus. *Nat Genet* 1994;7:383-9.
- Vance KW, Carreira S, Brosch G, Goding CR. Tbx2 is overexpressed and plays an important role in maintaining proliferation and suppression of senescence in melanomas. *Cancer Res* 2005;65:2260-8.
- Sherr CJ. The INK4a/ARF network in tumour suppression. *Nat Rev Mol Cell Biol* 2001;2:731-7.
- Jacobs JJ, Kieboom K, Marino S, DePinho RA, van Lohuizen M. The oncogene and Polycomb-group gene bmi-1 regulates cell proliferation and senescence through the ink4a locus. *Nature* 1999;397:164-8.
- Gil J, Bernard D, Martinez D, Beach D. Polycomb CBX7 has a unifying role in cellular lifespan. *Nat Cell Biol* 2004;6:67-72.
- Jacobs JJ, Keblusek P, Robanus-Maandag E, et al. Senescence bypass screen identifies TBX2, which represses Cdkn2a (p19(ARF)) and is amplified in a subset of human breast cancers. *Nat Genet* 2000;26:291-9.
- Lingbeek ME, Jacobs JJ, van Lohuizen M. The T-box repressors TBX2 and TBX3 specifically regulate the tumor suppressor gene p14ARF via a variant T-site in the initiator. *J Biol Chem* 2002;277:26120-7.
- Hanahan D, Weinberg RA. The hallmarks of cancer. *Cell* 2000;100:57-70.
- Kamijo T, Zindy F, Roussel MF, et al. Tumor suppression at the mouse INK4a locus mediated by the alternative reading frame product p19ARF. *Cell* 1997;91:649-59.
- Lowe SW, Sherr CJ. Tumor suppression by Ink4a-Arf: progress and puzzles. *Curr Opin Genet Dev* 2003;13:77-83.
- Pomerantz J, Schreiber-Agus N, Liegeois NJ, et al. The Ink4a tumor suppressor gene product, p19Arf, interacts with MDM2 and neutralizes MDM2's inhibition of p53. *Cell* 1998;92:713-23.